ANALYSIS OF HIGH RADIATION EFFICIENCY ULTRA WIDE BAND BOWTIE ANTENNA FOR IDENTIFICATION OF TUMOR CELLS

Rathanasabhapathy G[1], Mohamed Hamil G[2], Nithish Kumar V[3], Prabhananthan E[4], Simin Fathima S[5].

Assistant Professor[1], Final Year Students[2, 3, 4, 5], Department of Electronics and Communication Engineering[1, 2,3,4,5,]
Nandha Engineering College, Erode, Tamil Nadu, India.

Abstract: In the clinical industry, antennas are crucial. In order to create a bio verbal exchange machine among clinical gadgets and outside gadgets for short-variety biotelemetry applications, antennas can both be implanted into the human frame or absolutely hooked up over the skin. The Ultra-Wide Band (UWB) Bowtie Antenna applied on this assignment is described handiest with the aid of using the attitude fashioned with the aid of using the separation of the 2 planar steel portions with the aid of using the radio nice and poor terminals. UWB Bowtie Antennas are regularly created with inside the 3.1 to 10.6 GHz frequency variety. The most frequency has been set to six GHz for utilization in clinical microwave imaging (MWI). The tissues with a great water content material had an antenna mirrored image coefficient that became much less than - 12dB. It has an above-common radiation performance of 80%. The offered antenna's ability became proven with the aid of using a MWI-technique image reconstruction from the measured data.

Index Terms—Microwave imaging (MWI), UWB antenna, Tumor cells.

I. INTRODUCTION

Magnetic resonance imaging (MRI), computed tomography (CT), and positron emission tomography (PET) are a number of the present day traditional imaging strategies which have been considerably studied with inside the preceding two decades as alternatives. The gain of MWI technology is their low operational cost. The MWI strategies rely upon electromagnetic (EM) wave publicity of the imaging area and detection of meditated and scattered EM waves at surfaces with numerous dielectric characteristics, usually with the usage of antenna arrays. Depending at the MWI method, a couple of reconstruction strategies may be used to interpret records approximately the EM waves that man or woman antenna factors have acquired so that you can test and display the vicinity of interest (ROI) in 3 dimensions. The characteristics of the antenna factors we hired had a widespread effect at the MWI system`s potential to reconstruct images. It is feasible to apply nonionizing radiation and associated structures in a compact and modest manner. The duration among the onset of a mind stroke and its remedy may be substantially shortened with the usage of MWI, which has the capability to be carried out correctly at once in ambulance trucks. This is critical so that you can do away with awful fitness outcomes and enhance affected person prognosis. Non-invasive temperature tracking at some point of hyperthermia therapy, wherein the goal tumour vicinity's temperature is artificially raised to a number of forty to forty four stages Celsius for as a minimum an hour, is any other capability use for MWI devices. The MWI method may be used to become aware of this temperature boom due to modifications with inside the dielectric characteristics. MWI structures result in new necessities for the antenna elements. Among UWB antennas which are appropriate for MWI at microwave frequencies are Vivaldi planar antennas, double ridged horn antennas, planar monopole and bowtie dipoles antennas. The planar Vivaldi antenna makes use of exponentially tapered antipodal hands to radiate electricity immediately to the tissue. This antenna turned into designed for the breast most cancers detection machine primarily based totally at the radar approach. Due to the very low relative permittivity of the breast (about $\varepsilon r = 6$), canola oil is used as an identical liquid. UWB ridged horn antennas have excessive radiation efficiency, and the backward and aspect radiation is suppressed. These ridged horn antennas are normally full of excessive permittivity material (e.g., ceramics) inserted in the antenna and lowering the antenna dimensions. The weight of the antenna is excessive and, because of its filling, is likewise hard to fabricate as compared with different eligible antennas for MWI. Planar UWB monopole antennas provide a low-value answer of the problem, as they're clean to fabricate. Planar monopoles do now no longer want an identical liquid due to the fact they may be located at the floor of the analysed tissue. However, the benefit of the simplicity of planar layout involves the disadvantage of electricity deliver with inside the aircraft of the monopole patch, which isn't always very suitable and makes the usage of the sort of monopole in an array hard from the array perspective. Furthermore, the radiation sample of the planar UWB monopoles varies pretty notably with frequency, which may also motive distortion with inside the time domain. Bowtie dipoles, commonly planar dipoles and its modifications, are easy to fabricate. The geometry is broadband and the antenna is absolutely attachable immediately to the tissue (the matching liquid isn't always needed). Compared with the horn and Vivaldi antennas, the bowtie antenna has a decrease radiation efficiency and is greater touchy to the encircling environment. Due to the excessive permittivity price of the muscle tissue, a better a part of the EM electricity is emitted towards the phantom, which improves the efficiency. However, the bowtie antenna calls for symmetrical feeding, that is normally appropriate handiest for a confined frequency range. This paper is to design an UWB bowtie antenna together with UWB balanced-to-unbalanced (balun) for mixed MT. In the primary step, we've got studied and as compared numerous feasible micro strip UWB baluns . The maximum promising balun became mixed with the bowtie antenna, whose dimensions have been minimized via way of means of adjusting the form of bowtie edges the usage of a numerical parametric study. In the following step, we numerically examined primary antenna parameters for antenna usability. We numerically examined antenna radiation performance and established that bowties palms are symmetrically fed via way of means of visualization of floor modern density and |E| disciplined

distributions. The sensitivity of the antenna to air gaps formation and the sign distortion of the UWB sign have been examined. We as compared the anticipated and measured mirrored image traits and unique absorption rate (SAR) distribution of synthetic UWB bowtie antenna on the phantom of various equal tissues (Section II-A4). Then, we equidistantly placed 8 synthetic UWB bowtie antennas into the MWI head device. The ability of this device to come across and reconstruct the dielectric inhomogeneity within the human head phantom the usage of an aggregate of radar and MT processes have been studied.

II. ANTENNA DESIGN

The antenna provided in this paper is meant for the biomedical MWI applications. MWI structures are primarily composed of an array of antennas which are connected to the place to be imaged. The antenna parameters affect the reconstruction/ imaging capacity of the whole device. The antenna utilized in UWB MWI device must fulfil more than one needs with inside the meant ultra-wide frequency band, which might be as follows. 1) Efficient transmission of Electromagnetic energy into the tissue—low reflection coefficient of the antenna, minimized radiation to the encompassing regions. 2) Adequate near-subject radiation patterns—huge beam width with inside the azimuth aircraft and acceptably slender beam width with inside the elevation plane. 3) Acceptable bodily dimensions of the antenna element. The dimensions of the antenna decide the widest variety of antennas that might be dispensed across the location to be imaged. According to our experience, the minimum wide variety of antennas for a success MWI of, i.e., head with first rate accuracy in 2-D is 8 (in unmarried ring arrangement). We estimate that as much as sixteen bowtie antennas may be placed to cowl the whole head location (in 3-D).

A. Methods—Antenna Design

In step one of the UWB bowtie antenna development, we designed the bowtie arms shape. Then, we created UWB balun, as a bowtie dipole is a symmet trical structure, and calls for balanced feeding. In the third step, we optimized the complete UWB bowtie antenna geometry to fulfil given overall performance requirements.

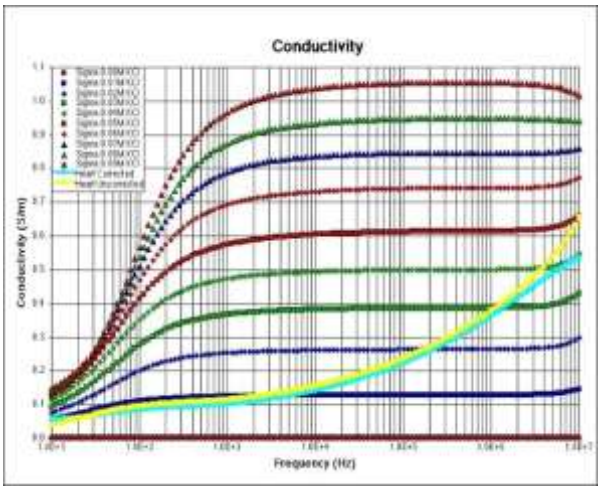

Fig. 1. Electrical conductivity of body tissues used in simulations that is of frequency band of 1–6 GHz.

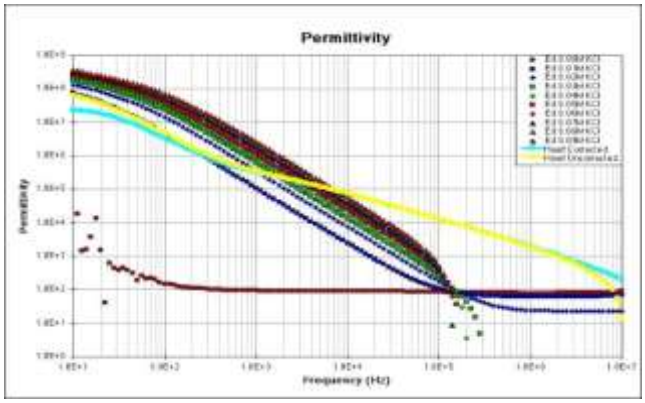

Fig. 2. Relative Permittivity of body tissues used in simulations which is connected to homogeneous Phantom.

In all numerical simulations, the antenna turned into at once connected to the homogeneous phantom with dielectric parameters being just like the precise human tissues (see Fig. 1 and 2). Fig. 1 indicates the electrical conductivity and Fig.2 indicates the relative permittivity of reviewed tissues with inside the entire simulated band, and information have been followed from the homogeneous phantom.

1) Bowtie Antenna Arms:

A bowtie antenna is a planar structure normally designed as a one-layer PCB. We examined the subsequent geometries, namely, "rounded bowtie antenna" (REBA), "triangle bowtie antenna with rounded corners" (TBARC), and fundamental "triangle bowtie antenna" (TBA) . All shapes have been derived from the TBA geometry with total length and width of 30 mm. Bowtie arms have been positioned at 1.524 mm peak substrate with dielectric properties. In the simulated antenna, the angle θ changed into constant to 45◦ collectively with balun confirmed the excellent reflection coefficient. The bowtie antenna overall performance is likewise depending on the dipole rounding radius R. The parametric examine has been accomplished to optimize the impedance matching of the proposed antenna over frequency band of interest.

2) UWB Balun:

UWB balun symmetric circuit is a key feature in the design of UWB antenna with symmetrical

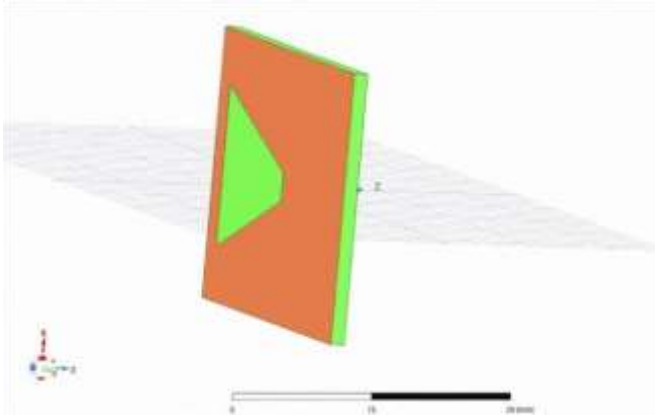

Fig. 3. Structure of Bowtie Arms.

Radiating pattern. The most applicable UWB balun solutions are ferrite or planar-tapered baluns. We decided to use the planar tapered UWB balun over ferrite baluns. This decision was based on assumption that the ferrites baluns can transform only limited RF power. According to our experience, the planar-tapered UWB baluns also cause lower UWB signal distortion at higher frequencies in comparison with the ferrite baluns. We calculated the strip widths of micro strip line and double sided parallel strip line (DSPSL) in a way to obtain 50 impedance at used 0.508 mm height Rogers RO4003C substrate. The balun length was set to 48 mm as a quarter of wavelength at 1 GHz. The width of the micro strip ground plane was set to wg = 25 mm. Four different balun shapes were considered, and the corresponding numerical models were created. The baluns were modelled as mirrored pairs with micro strip line at both ends and the DSPSL in the middle (in total 2 × 48 mm2 long). Geometries of the baluns are shown in Fig. 3. For all balun versions, S-parameters were calculated in the frequency band of 0.2–6 GHz. The antenna for the medical MWI should be directly attachable to the imaged area. If this option is to be maintained, then it is convenient to feed the bowtie dipole in a direction perpendicular to the plane of the dipole arms.

3) Simulation of Antenna Properties:

The following experiments were designed to clarify UWB antenna parameters, such as antenna usability for MWI of different tissues, antenna sensitivity to lower phantom contact to tissue, antenna radiation efficiency, and antenna radiation symmetry. First, a simple numerical model consists of a UWB antenna surrounded by a sphere of a radius of 20 cm where the front hemisphere was defined as the brain phantom. To acquire further insight into antenna performance, we have studied the current distribution over the surface of the bowtie arms. The current distribution was visualized using vectors to prove the ability of the balun to provide sufficient symmetric feeding of the bowtie arms. Second, we evaluated the radiation efficiency of the antenna. The introduced antenna is intended to operate in a lossy medium (average human brain phantom) in the near-field antenna region. To express the antenna radiation efficiency to the human brain phantom, the parameter E f was introduced. The parameter E f was calculated according to the following equation:

$$E_f = \frac{P_{head}}{P_{in}} \cdot 100(\%) \quad (1)$$

Where Pin (W) is the input power, and Phead (W) is the power absorbed in the brain phantom in front of the antenna. The method of radiation patterns, with respect to antenna theory. It is hardly applicable for some cases. Instead, we proposed to evaluate SAR (W/kg) in yz plane for frequency range 1–6 GHz with a 2 GHz step. The numerically obtained SAR was normalized by the maximum value and compared with the measured SAR. The boundary conditions of the model were set to scattering boundary conditions that suppress reflections. We further numerically evaluated the normalized magnitude of the intensity of the electric field intensity |E| depending on the radiation angle (◦) in xz and yz planes (H- and E-planes). The electric field intensity was computed for the frequencies 1, 3, and 5 GHz in both planes perpendicular to the antenna. The evaluation angle ranged from −90◦ to 90 ◦ with respect to the antenna position. The transition between brain and air hemisphere stands for 0◦ angle.

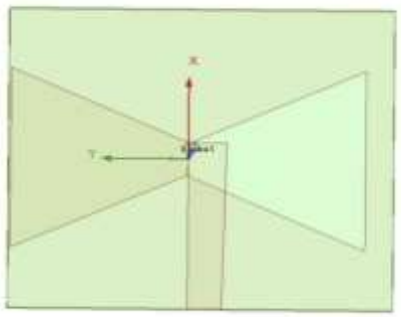

Fig. 4 . Design of Bowtie Antenna w.r.t Global Axis.

Furthermore, the antenna medical versatility was verified numerically and experimentally via the comparison of the reflection parameters. The UWB signal that is emitted and which is propagating through lossy media (i.e., human tissues) is attenuated. This attenuation is frequency dependent and affects the signal amplitude and signal shape. To eliminate this effect, and only for this signal distortion study, the phantom electrical conductivity was set to 0 (S/m). Thus, we can observe just signal distortion caused by antenna element itself. One antenna was determined as transmitting (Tx) one. It emits the UWB Gaussian pulse of the frequency band of 1–6 GHz. The opposite antenna was in the receiving mode (Rx). The most common parameter for UWB signal distortion evaluation is fidelity, which is calculated as a cross correlation between the normalized Tx and Rx signals. The fidelity factor F (-) is defined as follows

$$F = max \frac{\int_{-\infty}^{+\infty} T(t)R(t+\tau)dt}{\sqrt{\int_{-\infty}^{+\infty}|T(t)^2|dt \int_{-\infty}^{+\infty}|R(t)^2|dt}} \quad (2)$$

Where T(t) is transmitted signal, R(t) is received signal, t is time, and τ is time displacement. The time domain signals from the proposed antenna are also compared with signals from previously used UWB bowtie antenna (for brain imaging) as well as the fidelity factor F.

Table. 1. Dimensions of the Designed Antenna.

ANTENNA DIMENSIONS	
INNER WIDTH (mm)	**20**
OUTER WIDTH (mm)	**40.1**
ARM LENGTH (mm)	**44.6**
PORT GAP WIDTH (mm)	**22**

Table.2. Dimensions of the Substrate.

SUBSTRATE DIMENSIONS	
MATERIAL	**FR4_epoxy**
SUBSTRATE HEIGHT (mm)	**15.75**
SUBSTRATE DIMENSIONS X(mm)	**180**
SUBSTRATE DIMENSIONS Y(mm)	**180**

III. UWB MICROWAVE HEAD IMAGING SYSTEM

A. Methods—MW Imaging System

The MWI system inclusive of Gauss–Newton MWI reconstruction method was formerly discussed. The system has been changed for an array of 8 UWB antennas. This was accomplished with appreciate to cross-coupling reduction amongst antennas. The variety of used antennas changed into decreased from 10 to 8 to increase the attitude among antennas and hence to lessen the antenna crosstalk. The dimensions of the field are 200 × 160 mm2 primarily based totally on common grownup male head. The antennas have been equidistantly positioned in a single ring with inside the plastic antenna holder to shape a multi static array across the place to be imaged. The field top is 200 mm top with 2 mm-thick wall. It includes the octagonal pins on the bottom that are used for particular phantoms positioning which represents inhomogeneity to be imaged. These cylindrical phantoms have a diameter of 40 mm. UWB bowtie antennas have been related to the switching matrix the usage of a semirigid coaxial cable.

a) Liquid Phantoms: Liquid phantoms have been used for all measurements for the reason that they

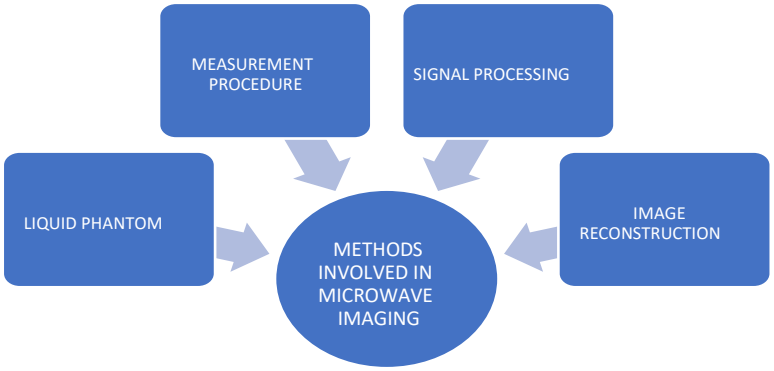

Fig. 5 . Methods Involved in Microwave imaging.

permit to connect the antenna without any air gaps and permit us to area preferred inhomogeneity to a predefined position. We organized phantom with the dielectric parameters of common human brain in step with the dielectric properties. The phantom turned into organized with the aid of using blending of deionized water and isopropyl alcohol. By converting the isopropyl alcohol and deionized water ratio, an extra phantom turned into organized, representing a small deviation in dielectric parameters (phantom relative permittivity εr turned into approximately +5%). Dielectric parameters have been extrapolated to the frequency band of our interest (0.5–6 GHz).

1) Measurement Procedure—MWI System: The field of MWI device became full of defined liquid brain phantom. The plastic cylinder full of inhomogeneity phantom, representing the inhomogeneity, became inserted in predefined position in field. Four positions of this cylinder have been measured to illustrate the potential of the MWI device to reconstruct 2-D scattering phantom profile, respectively, and the potential to stumble on inhomogeneity inside the analysed region. The following size parameters have been set: frequency bandwidth of 1–6 GHz, VNA output power of 13 dBm, and intermediate frequency bandwidth of 100 Hz.

2) Signal Processing and Image Reconstruction:

a) Radar approach: The resulting frequency area statistics had been converted into the time area the usage of inverse discrete Fourier transform (IDFT). Thus, the device impulse reaction matrix was received. Time shift T(dm) for every captured sign and every focal factor r0 become calculated through estimating propagation velocity vp of the EM wave in measured tissue with dielectric constant εr and from recognised round-trip distance dm of transmitting antenna, of particular, investigated focal point and receiving antenna.

$$T(d_m) = \frac{d_m}{v_p}, \; v_p = \frac{c}{\sqrt{\varepsilon_r(f)}} \qquad (3)$$

Wherein c (m/s) is velocity of light and ε_r is a relative permittivity of phantom at vital frequency of measured bandwidth. The "Delay and Sum" algorithm and its set of rules become used for the inhomogeneity function reconstruction. By making use of this procedure, 2-D power profile displaying scattering/reflecting regions become created. The intensity I(r0) especially focal factor can be obtained by the equation,

$$I(r_0) = \sum_{t=-\frac{T_\omega}{2}}^{\frac{T_\omega}{2}} \sum_{m=1}^{\frac{N(N+1)}{2}} \left(\omega_m(d_m) \cdot \Delta x_m\left(t + T(d_m)\right)\right)^2 \qquad (4)$$

Where Tw is a predefined time-window and w_m is a weighting factor for path dependent attenuation, t is time, N is number of channels, and x_m is a differential signal that is calculated by the equation,

$$\Delta x_m(t) = |s_i(t)| - |s_w(t)| \qquad (5)$$

Where s_i is a signal measured when the inhomogeneity phantom was present, and s_w is a signal measured without inhomogeneity phantom. The signals received by the antennas with an internal angle wider than 90◦ to the transmitting antenna is neglected as they usually do not improve the final image quality.

b) MT approach: To exhibit MT approach, we carried out differential MT algorithm for non-invasive microwave thermometry. This algorithm exploits born approximation (BA) with regularization via means of truncated singular value decomposition (TSVD) to reconstruct differential dielectric profile of brain phantom with inhomogeneity positioned inside.

c) Hybrid approach: The mixture of radar and MT technique can optimize the procedure of image reconstruction in terms of pace and accuracy. We can break up the procedure into steps. First, from the outcomes received from the radar primarily based totally technique, the algorithm identifies the ROI wherein the inhomogeneity in the device is placed. Complex permittivity reconstruction the usage of differential MT technique with BA and TSVD regularization is sensitive on artifacts with inside the ensuing picture. Usually one or extra fake reconstructed "hot spots" may be observed. Therefore, the actual function of inhomogeneity will be tough to perceive and additionally decrease range of truncation level needs to be applied. It results to distortion of reconstructed values of differential dielectric parameters.

B. Tomography Technique

A moving x-ray tube fades the structure of malignant cells in the tomography x-ray technique. While cross-sectional imaging methods like US, CT, and MRI are now available, conventional tomography is being utilized less frequently. Tomography can be divided into two categories: linear and nonlinear. Both methods revolve around a fulcrum, with the tube moving in one direction and the film cassette moving in the opposite direction. By using computer processing, a computed tomography (CT) scan creates cross-sectional images of the bones, blood arteries, and soft tissues within your body by combining a number of Xray images collected from various angles all over your body. Images from a CT scan offer more information than an X-ray would.

Table.3.Electrical Conductivity and Relative Permittivity of Different Body Tissues.

Tissue	ε_r	σ (S/m)	Tissue	ε_r	σ (S/m)
Mean-head tissue	43.5	0.87	Fat	11.62	0.08
Mean-body tissue	56.7	0.94	Kidney	66.32	1.09
Bone	13.14	0.09	Liver	51.18	0.65
Brain-grey-matter	57.37	0.74	Lung	23.79	0.37
Brain-white-matter	42.03	0.44	Muscle	57.10	0.79
Cerebellum	55.91	1.03	Skin	46.72	0.69
Cerebrospinal fluid	70.96	2.25	Skull/Vertebrae	13.14	0.09
Eye lens	37.48	0.37	Stomach	67.46	1.00

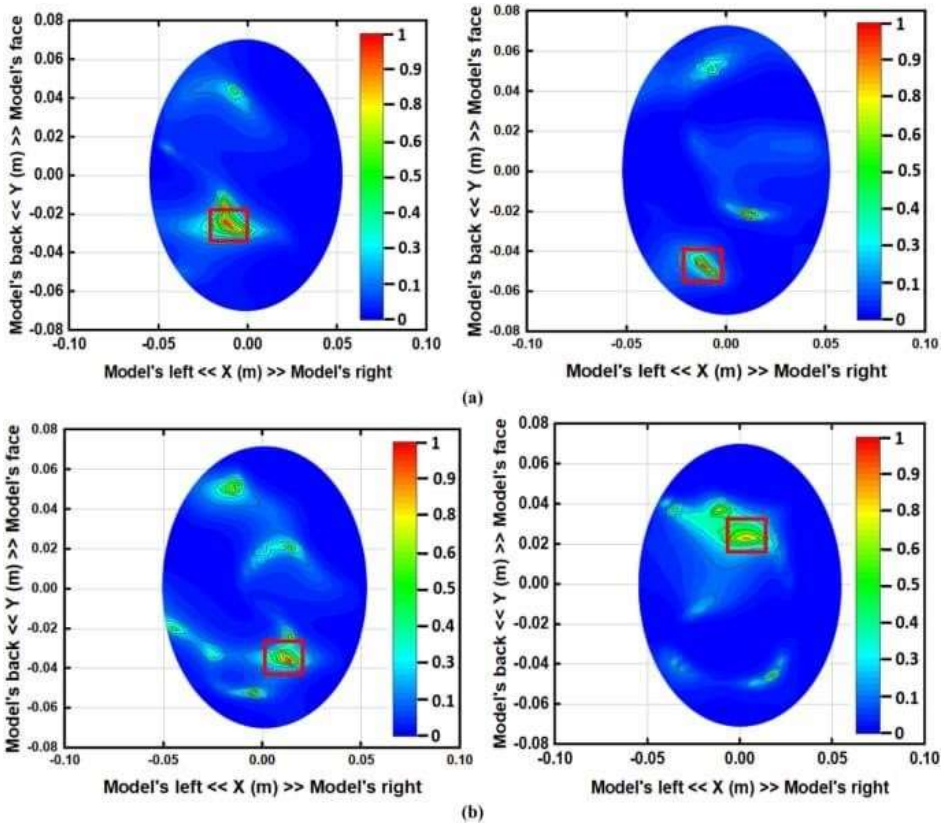

Fig. 6. Reconstructed scattering profile (normalized intensity |I|) of liquid brain phantom with inserted cylindrical-shaped dielectric inhomogeneity. The position (P1–P4) of the inhomogeneity is marked by the red square.

IV. DISCUSSION

The UWB bowtie antenna for application in UWB MWI structures became designed and its calculated traits showed with the aid of using collection of numerical simulations and measurements. Bowtie arms have been miniaturized with the aid of using facet rounding that's useful in MWI structures with better range of antennas. Smaller dipole arms dimensions have a wonderful impact at the antenna impulse reaction. We designed the UWB balun which gives enough reflection coefficient (|S11| < −10 dB) in its complete frequency band (1– 6 GHz) whilst linked to the bowtie dipole arms. Here, the provided UWB antenna stands proud above the opposite UWB antennas designed for MWI especially with inside the extensive usable frequency bandwidth (3–6 GHz) which gives enough decision for maximum biomedical utility of MWI. To show this statement, the very last antenna detail became connected to numerous varieties of tissues and the |S11| parameter became simulated. The simulation outcomes display that the antenna is absolutely functional (|S11| < −10 dB) in its complete frequency band (3–6 GHz) for tissues which have better water content (mind and muscle). For pores and skin tissue, the frequency band reduced barely to 3–5 GHz. For tissues (bone tissue in our case) with low water content, we consider that the frequency band continues to be beneficial among 3 and 4 GHz. The anticipated UWB bowtie antenna |S11| function became showed with the aid of using dimension with the aid of using the usage of muscle and brain phantom (in the imaging machine) with inside the 3–6 GHz frequency band with value properly below 12 dB with inside the complete studied frequency band. The fractional bandwidth of the designed antenna is 143%. The fractional bandwidth is one of the maximum values which may be determined with inside the literature. This guarantees brief impulse reaction of the antenna. Some antennas gives better fractional bandwidth that is 163% with similar constancy thing and is designed for the pinnacle imaging. Our UWB antenna possesses a excessive radiation efficiency (over 80% with inside the complete frequency band) to the brain phantom and, therefore, does now no longer be afflicted by excessive backward radiation. The antennas with excessive efficiency are capable of transmit better energy and for this reason come across decrease dielectric adjustments. Simulated and measured SAR distributions in addition to |E| discipline distribution with inside the mind phantom of the proposed antenna proven symmetrical radiation pattern. Final antenna dimensions are 60 × 60 × 50 mm3. The front panel of dimensions 60 × 60 mm2 became selected as suitable for insertion to the mind imaging machine formerly evolved in our laboratory. However, the simulation of the antenna sensitivity to air gaps among antenna and brain phantom confirmed that with inside the presence of air beneath energetic part (metal bowties), the antenna overall performance is low and, therefore, utility of matching liquid is required. If the air hole is out of doors the antenna energetic area, that air hole has no or very low impact on |S11|. The constancy thing for brain phantom became 0.81, for pores and skin 0.79, and for muscle 0.83. In case of bone tissue, the constancy became decrease (0.70).Due to the huge UWB bandwidth, the constancy thing is decrease as compared with the antennas formerly published (constancy thing degrees from 80% to 92%). This guarantees that provided antenna has minimum time area distortion of the Tx/Rx signals. Developed UWB bowtie antenna became carried out in 8 channel microwave UWB imaging machine. Results confirmed superb detectability of the inhomogeneity function inside head phantom with the aid of using the radar technique. The ROI became decided on the usage of reconstructed facts from the radar technique. This ROI became used as an enter a priori statistics to MT technique primarily based totally on BA. This brought about an improved accuracy of the reconstruction in addition to filtering of undesirable hotspots. The reconstruction system became additionally sped up with the aid of using about 20% because of decreasing the research area best on ROI. The reconstruction of measured facts primarily based totally on electric conductivity profile became distorted and now no longer absolutely successful. It may be as a result of too excessive truncation stage. Since the conductivity adjustments have been in orders of tenths, the steadiness of the set of rules may be oversaturated. Reduction of truncation stage could cause lower of reconstructed assessment accuracy of relative permittivity facts. Increasing the antennas quantity and its positions in exceptional rings can cause higher reconstruction accuracy. The scattering profile reconstruction indicates that still for terribly low change in dielectric parameters permitting the machine to as it should be come across the stroke. The direction of Electric and Magnetic field vector of the designed antenna is shown in the figure 7 and 8.

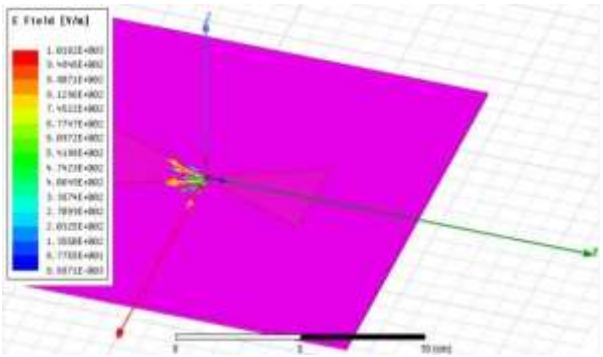

Fig. 7.Direction of Electric Field.

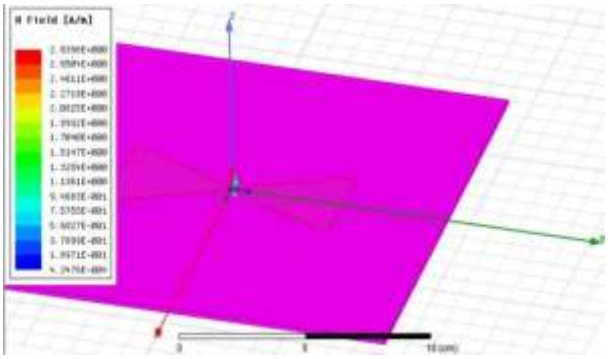

Fig. 10 .Direction of Magnetic Field.

V.OBSERVATION

The designed UWB Bowtie Antenna designed at a centre frequency of 4.5 GHz to perform medical microwave imaging for the identification of Tumour cells shows the following characteristics,

DIELECTRIC SUBSTRATE USED	Epoxy FR4
PEAK GAIN	5 dB
PEAK DIRECTIVITY	4.9 dB
RADIATION EFFICIENCY	0.98
BANDWIDTH	3-6 GHz
RADIATION PATTERN	Symmetrical, Omnidirectional
VSWR	<=2.5
DIELECTRIC CONSTANT OF THE SUBSTRATE	4.8

VI. CONCLUSION

In this work, the design of an UWB antenna for MWI is provided, and its suitability is experimentally verified. The provided UWB antenna indicates a excessive radiation efficiency (above 80%) and a symmetrical radiation sample with inside the entire operating frequency band. The beneficial frequency band may be very wide (3–6 GHz) which lets in the antenna for use for maximum MWI applications providing excessive spatial resolution. The constancy component over 80% guarantees true antenna capability with low distortion and true impulse response. The antenna parameters, including true |S11|, operating frequency band, and radiation efficiency, are critical for the sensitivity of the reconstruction algorithms. Our antenna has fulfilled all parameters cited above with inside the entire UWB band. The compactness of the antenna predestines it for MWI structures with a better range of antenna elements, and the development of the antenna then permits reasonably priced and repeatable manufacturing via way of means of mounted strategies of manufacturing of published circuit boards. The antenna can consequently be used as the idea for greater correct MWI multifrequency structures and also can be carried out in UWB MWI hybrid.

VII. REFERENCES

1. O. Fiser et al., “UWB Bowtie Antenna for Medical Microwave Imaging Applications,” in IEEE .Transactions on Antennas and Propagation, vol. 70, no. 7, pp. 5357-5372, July 2022, doi: .10.1109/TAP.2022.3161355.
2. C. H. S. Nkimbeng, H. Wang and I. Park, “Low-Profile Wideband Unidirectional Circularly .Polarized MetasurfaceBased Bowtie Slot Antenna,” in IEEE Access, vol. 9, pp. 134743-134752, .2021, doi: 10.1109/ACCESS.2021.3116714.
3. M. Alibakhshikenari et al., “Dual-Polarized Highly Folded Bowtie Antenna With Slotted Self .Grounded Structure for Sub-6 GHz 5G Applications,” in IEEE Transactions on Antennas and .Propagation, vol. 70, no. 4, pp. 3028-3033, April 2022, doi: 10.1109/TAP.2021.3118784.

4. G. Yang, S. Ye, Y. Ji, X. Zhang and G. Fang, "Radiation Enhancement of an Ultrawideband .Unidirectional Folded Bowtie Antenna for GPR Applications," in IEEE Access, vol. 8, pp. 182218-.182228, 2020, doi: 10.1109/ACCESS.2020.3029050.
5. P. Khanal, J. Yang, M. Ivashina, A. Höök and R. Luo, "A Wide Scanning Array of Connected .Bowtie Antennas Suitable for Integration in Composite Sandwich Structures With MonteCarlo .Tolerance Analysis," in IEEE Access, vol. 9, pp. 146691-146702, 2021, doi: .10.1109/ACCESS.2021.3123439.
6. H. Yu, S. Fang, L. Jiang and H. Liu, "A Full-Band Digital Television Transmitting Antenna Array .With Dual-Layer Bowtie Dipole Unit," in IEEE Access, vol. 8, pp. 102138- 102145, 2020, doi: .10.1109/ACCESS.2020.2998516.
7. K. Schmalz et al., "Dual-Band Transmitter and Receiver With Bowtie-Antenna in 0.13 µm SiGe .BiCMOS for Gas Spectroscopy at 222 – 270 GHz," in IEEE Access, vol. 9, pp. 124805-124816, 2021, .doi: 10.1109/ACCESS.2021.3110210.
8. W. van Verre et al., "Reducing the Induction Footprint of Ultra-Wideband Antennas for Ground-.Penetrating Radar in Dual-Modality Detectors," in IEEE Transactions on Antennas and Propagation, .vol. 69, no. 3, pp. 1293-1301, March 2021, doi: 10.1109/TAP.2020.3026909.
9. D. H. Nguyen, J. Stindl, T. Slanina, J. Moll, V. Krozer and G. Zimmer, "High Frequency Breast .Imaging: Experimental Analysis of Tissue Phantoms," in IEEE Open Journal of Antennas and .Propagation, vol. 2, pp. 1098-1107, 2021, doi: 10.1109/OJAP.2021.3127653.
10. Q. Liu, H. Liu, W. He and S. He, "A Low-Profile DualBand Dual-Polarized Antenna With an .AMC Reflector for 5G Communications," in IEEE Access, vol. 8, pp. 24072-24080, 2020, doi: .10.1109/ACCESS.2020.2970473.
11. K. Schmalz, A. Glück, N. Rothbart, A. Güner, M. H. Eissa and H. -W. Hübers, "Transmitter and .Receiver in 0.13 µm SiGe for Gas Spectroscopy at 222–270/444–540 GHz," in IEEE Journal of .Microwaves, vol. 2, no. 4, pp. 582-591, Oct. 2022, doi: 10.1109/JMW.2022.3194062.
12. R. Xiao, W. Geyi and W. Wu, "Theory of Resonant Modes and its Application," in IEEE Access, .vol. 9, pp. 114945-114956, 2021, doi: 10.1109/ACCESS.2021.3105194.
13. Y. -F. Wang, B. Wu, N. Zhang, Y. -T. Zhao and T. Su, "Wideband Circularly Polarized .Magneto-Electric Dipole 1×2 Antenna Array for Millimeter-Wave Applications," in IEEE .Access, vol. 8, pp. 27516-27523, 2020, doi: 10.1109/ACCESS.2020.2971860.
14. A.A. Omar, A. Mahmoud, J. Choi and W. Hong, "Wideband Transmissive Polarization Rotator .With In-Band Notches Enabling Multiband Operation," in IEEE Access, vol. 9, pp. 44751-44756, .2021, doi: 10.1109/ACCESS.2021.3066638.
15. P. -Y. Feng, S. -W. Qu, X. -H. Chen and S. Yang, "LowProfile High-Gain and Wide-Angle .Beam Scanning Phased Transmitarray Antennas," in IEEE Access, vol. 8, pp. 34276- 34285, 2020, .doi: 10.1109/ACCESS.2020.2974066.
16. T. T. Le, Y. -D. Kim and T. -Y. Yun, "Wearable PatternDiversity Dual-Polarized Button .Antenna for Versatile On- /Off-Body Communications," in IEEE Access, vol. 10, pp. 98700-98711, .2022, doi: 10.1109/ACCESS.2022.3206799